

An Envelope Alignment Method for Terahertz Radar ISAR Imaging of Maneuvering Targets

Tong Liu, Zongjie Cao and Rui Min

Abstract A novel envelope alignment technique for terahertz radar ISAR imaging of maneuvering targets is presented in this paper. This method selects a single pulse echo as the envelope alignment benchmark through the correlation coefficient of adjacent range profiles, which solves the problems of jump error and drift error in the conventional adjacent amplitude correlation method. The imaging results of measured terahertz data demonstrate the effectiveness of this improved envelope alignment technique based on the adjacent amplitude correlation method.

Keywords Terahertz radar · Maneuvering targets · Envelope alignment · ISAR imaging

1 Introduction

As terahertz wave can penetrate nonpolar materials and has a strong reflect character towards metal materials, and is easy to achieve large bandwidth modulated signal, terahertz radar can obtain high resolution images of concealed threats, such as knives and guns hidden in clothing or luggage. Meanwhile, due to the low photon energy, terahertz wave is harmless to human body. It is an attractive technology to do the security checks and the monitoring of concealed threats at a standoff range utilizing terahertz radar nowadays [1, 2]. Considering the practical application demands and the convenience requirements, the research on terahertz radar ISAR imaging of maneuvering targets is necessary.

The relative motion between maneuvering targets and radar can be divided into the translation component and the rotation component. The translation component

T. Liu (✉) · Z. Cao · R. Min

School of Electronic Engineering, University of Electronic Science and Technology of China, Chengdu, China
e-mail: liutong013@163.com

makes no contribution to ISAR imaging, but it will cause range cell migration and Doppler variation to degrade the imaging quality. The impact of the translation component should be eliminated by envelope alignment and phase correction before imaging. Envelope alignment is the base of phase correction and imaging. Because terahertz wave has a shorter wavelength than microwave or millimeter wave, the rotation angle that terahertz radar ISAR imaging required is smaller, for which the envelope of terahertz radar echo is very similar. Traditionally, the adjacent amplitude correlation method can gain a good envelope alignment effect, but it has the jump error and drift error problems [3] which would cause the terahertz radar image defocusing.

An improved envelope alignment technique based on the adjacent amplitude correlation method is presented in this paper. The single pulse echo is sifted as the envelope alignment benchmark through the correlation coefficient of adjacent range profiles, and the problems of jump error and drift error in the conventional adjacent amplitude correlation method are solved. The imaging results of measured terahertz data demonstrate the effectiveness of this improved envelope alignment method.

2 Theory and Methodology

2.1 Received Signal Model

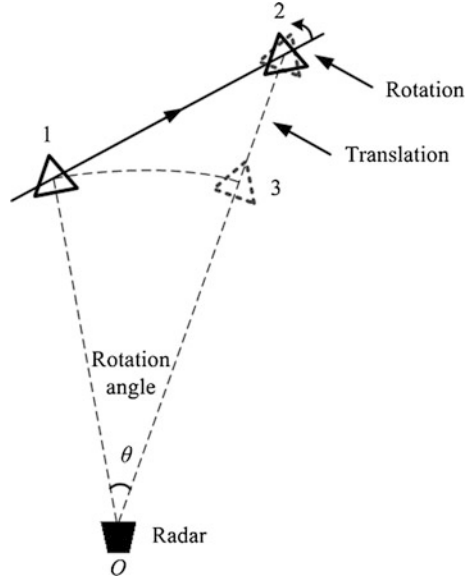
The relative motion between maneuvering targets and radar can be divided into the translation component (Maneuvering targets move from point 3 to point 2) and the rotation component (Maneuvering targets rotate from dotted line position to solid line position at point 2), as shown in Fig. 1. Since the rotation angle that terahertz radar ISAR imaging required is small, the rotation velocity is approximately uniform. After eliminating range cell migration and Doppler variation that the translation component caused by envelope alignment and phase correction, the ISAR imaging of maneuvering targets will be converted into the basic concepts of Range-Doppler imaging for ISAR [4].

Terahertz radar transmits line frequency modulation signal with the pulse repetition interval T . The transmitted signal can be expressed as

$$s(\hat{t}, t_m) = \text{rect}\left(\frac{\hat{t}}{T_p}\right) e^{j2\pi(f_c t + \frac{1}{2}\gamma t^2)} \quad (1)$$

where $\text{rect}(u) = \begin{cases} 1 & |u| \leq \frac{1}{2} \\ 0 & |u| > \frac{1}{2} \end{cases}$, T_p is the pulse width, f_c is the center frequency, γ is the chirp rate of the transmitted signal. The moments at which the signal is transmitted $t_m = mT$ ($m = 0, 1, 2, \dots$) are called slow time. \hat{t} denotes the time variable varying

Fig. 1 ISAR imaging geometry of maneuvering targets



within the pulse repetition interval, which is called fast time. The relationship between t_m and \hat{t} is $\hat{t} = t - mT$.

Assume that the maneuvering target is an ideal geometric point, the instantaneous distance between the maneuvering target and the radar is $R(t_m)$ at t_m . The received signal reflected from the maneuvering target can be denoted as

$$s_r(\hat{t}, t_m) = A \text{rect}\left(\frac{\hat{t} - 2R(t_m)/c}{T_p}\right) e^{j2\pi\left(f_c\left(t - \frac{2R(t_m)}{c}\right) + \frac{1}{2}\gamma\left(\hat{t} - \frac{2R(t_m)}{c}\right)^2\right)} \quad (2)$$

where A denotes the echo signal amplitude and c is the speed of light. The intermediate frequency signal can be expressed as

$$\begin{aligned} s_{if}(\hat{t}, t_m) &= s_r(\hat{t}, t_m) \cdot s^*(\hat{t}, t_m) \\ &= A \text{rect}\left(\frac{\hat{t} - 2R(t_m)/c}{T_p}\right) e^{-j\frac{2\pi}{c}f_c R(t_m)} e^{-j\frac{2\pi}{c}\gamma R(t_m)} e^{j\frac{2\pi}{c^2}R^2(t_m)} \end{aligned} \quad (3)$$

Applying the Fourier transform to $s_{if}(\hat{t}, t_m)$ with variable \hat{t} and removing the residual video phase and envelope migration phase, the expression of the radar echo in frequency domain becomes

$$S_{IF}(f_i, t_m) = AT_p \text{sinc}\left[T_p\left(f_i + 2\frac{\gamma}{c}R(t_m)\right)\right] e^{-j\frac{2\pi}{c}f_c R(t_m)} \quad (4)$$

2.2 ISAR Imaging of Maneuvering Targets

$u(i), i = 1, 2, \dots, M-1$ is the correlation coefficient of adjacent range profiles of radar data $A(m, n)$, where $m(m = 1, 2, \dots, M)$ denotes sequence of azimuth, $n(n = 1, 2, \dots, N)$ denotes range cell. L samples are taken from $u(i)$ as a group in turn and their mean is computed. The one whose mean is maximal in those groups is picked out

$$K = \max_{1 \leq i \leq M-L} \left\{ \frac{1}{L} \cdot [u(i) + u(i+1) + \dots + u(i+L-1)] \right\} \quad (5)$$

where K is the index of groups.

The single pulse echo corresponding to the maximal correlation coefficient of adjacent range profiles in the K th group is selected as the envelope alignment benchmark.

$$J = \max_{K \leq j \leq K+L-1} \{u(j)\} \quad (6)$$

$A(J, n)$ is the unity benchmark of envelope alignment. The cross-correlation function of $A(m, n)$ and $A(J, n)$ is

$$R_{mJ}(\tau) = \sum_{\tau=0}^N A(m, n)A(J, n-\tau) \quad (7)$$

After searching for the peak and computing the range cells corresponding to τ , the envelope alignment is completed. In order to achieve high accuracy requirement for envelope alignment, the range cell is processed with a 16-time interpolation before the cross-correlation function is computed.

The focused image makes the entropy of image minimal, which is the principle of phase correction based on the minimum entropy method [5].

$f(m, n)$ denotes the signal after envelope alignment. Applying the Fourier transform to the result of $f(m, n)$ multiplying the phase correction term, the image is obtained.

$$\begin{aligned} g(k, n) &= \text{fft}[f(m, n) \cdot \exp[\phi(m)]] \\ &= \sum_{m=0}^{M-1} f(m, n) \cdot \exp[\phi(m)] \cdot \exp\left(-j \frac{2\pi}{M} km\right) \end{aligned} \quad (8)$$

where k denotes the Doppler frequency index, $\phi(m)$ is the correction phase.

Ignoring the constant term, the entropy of image is defined as

$$\varepsilon \left[|g(k, n)|^2 \right] = \sum_{k=0}^{M-1} \sum_{n=0}^{N-1} |g(k, n)|^2 \ln |g(k, n)|^2 \quad (9)$$

When the entropy of image is minimal, the correction phase $\phi(m)$ satisfies the following condition:

$$\frac{\partial \varepsilon \left[|g(k, n)|^2 \right]}{\partial \phi(m)} = 2M \operatorname{Im} \left\{ \exp[j\phi(m)] a^*(m) \right\} = 0 \quad (10)$$

where $a(m) = \sum_{n=0}^{N-1} f^*(m, n) \cdot \frac{1}{M} \sum_{k=0}^{M-1} \left[1 + \ln |g(k, n)|^2 \right] g(k, n) \exp(j \frac{2\pi}{M} km)$.

Therefore,

$$\phi(m) = \arg[a(m)] \quad (11)$$

The correction phase $\phi(m)$ can be estimated by iterative process. The termination condition for the iteration is

$$\max_{m=0}^{M-1} \{ |\exp[j\phi_i(m)] - \exp[j\phi_{i-1}(m)]| \} \leq \mu \quad (12)$$

where $\phi_i(m)$ and $\phi_{i-1}(m)$ are the values of $\phi(m)$ in current iteration and last iteration, respectively. μ is a constant decided by the accuracy of $\phi(m)$.

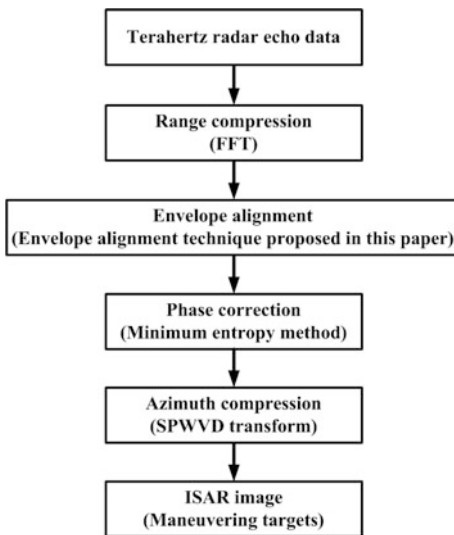
Because the phase error still exists after the translation compensation, and the velocity of the small angle rotation is approximately uniform but not strictly uniform, the image obtained by applying Fourier transform to the azimuth of the signal after the translation compensation is defocusing. The time-frequency transform instead of the Fourier transform is used for the ISAR imaging of maneuvering targets to make image focus [6]. Due to the multiple scattering points, the smoothed pseudo Wigner Ville distribution (SPWVD) is selected for imaging.

$$SPWVD_s(t, \omega) = \int h(t') \int g(u) \cdot s(t - u + \frac{t'}{2}) s^*(t - u - \frac{t'}{2}) du e^{-j\omega t'} dt' \quad (13)$$

where $s(t)$ denotes any signal, $g(t)$ and $h(t)$ are the time-domain window function and the frequency-domain window function, respectively. The SPWVD suppresses cross-term interference at the expense of the time resolution and the frequency resolution.

The flow chart of terahertz radar ISAR imaging of maneuvering targets is shown in Fig. 2.

Fig. 2 Flowchart of ISAR imaging of maneuvering targets



3 Experiment and Results

The terahertz radar system works at 0.34 THz with a bandwidth of 10.08 GHz, which leads to a range resolution of 1.5 cm [7]. The image of the terahertz radar is shown in Fig. 3a. The maneuvering target consists of two corner reflectors inlaid on the foam board, as shown in Fig. 3b. The foam board slides within the scope of the radar beam at a distance of 10 m off the radar by the fine line traction.

2800 radar pulse echoes are collected and the accumulation angle of azimuth is about 1.7°, which leads to an azimuth resolution of 1.5 cm matched to the range

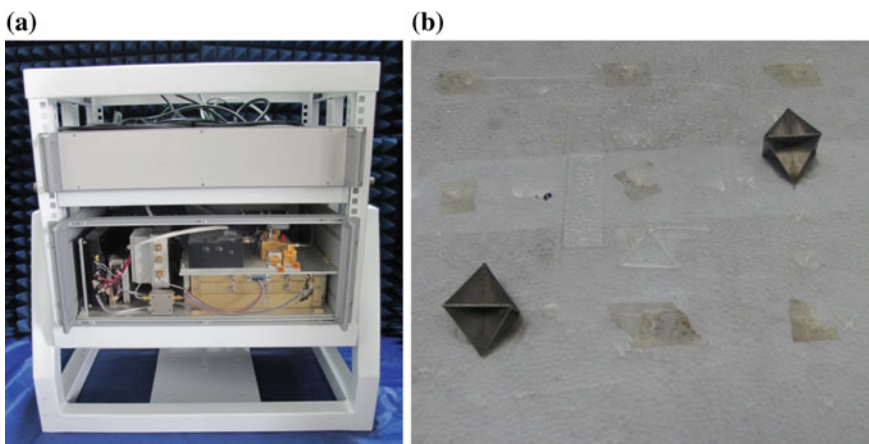


Fig. 3 Image of the terahertz radar and the maneuvering target. **a** Image of the terahertz radar. **b** Maneuvering target

resolution. The envelope of the radar echoes after range compression is shown in Fig. 4a. The translation component leads to range cell migration. The envelope after envelope alignment via the adjacent amplitude correlation method is shown in Fig. 4b. The ISAR image is shown in Fig. 4c with the SPWVD in azimuth imaging. The correlation coefficient of adjacent range profiles of the terahertz radar data is

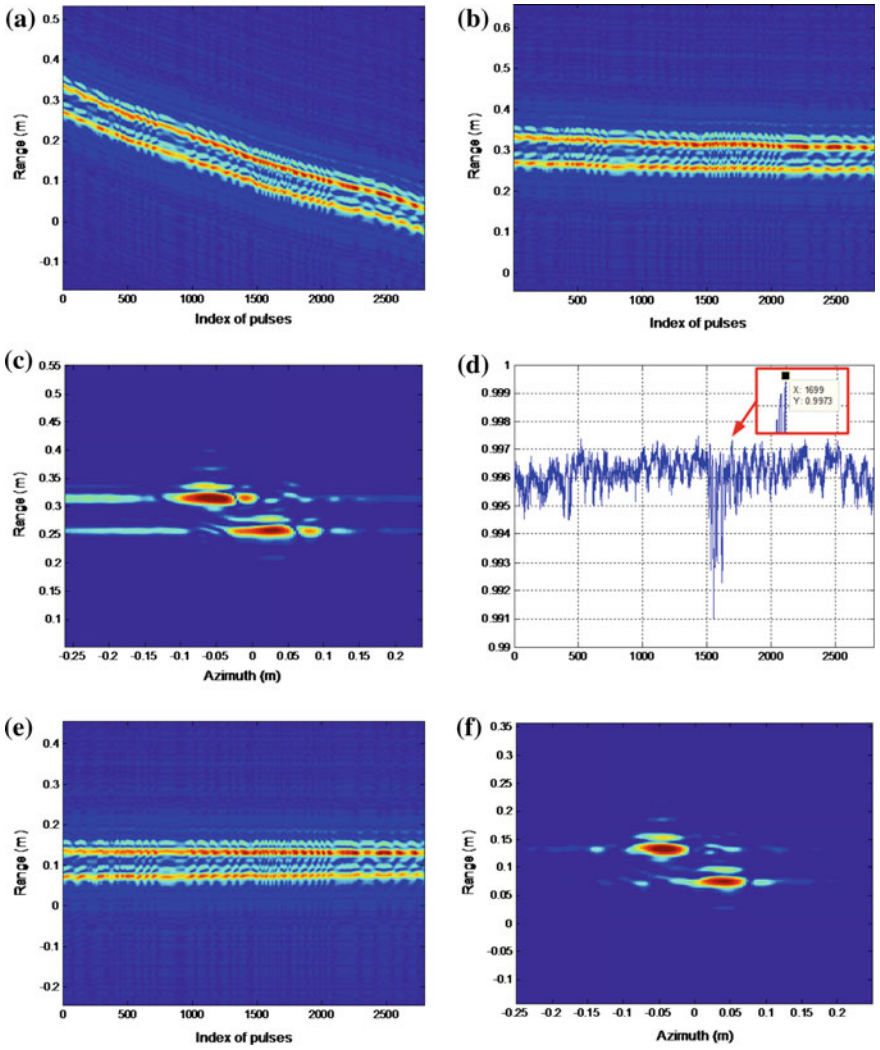


Fig. 4 ISAR imaging of maneuvering target. **a** Envelope after range compression. **b** Envelope after envelope alignment via the adjacent amplitude correlation method. **c** ISAR image gained via azimuth SPWVD transform. **d** The correlation coefficient of adjacent range profiles. **e** Envelope after envelope alignment via the envelope alignment technique proposed in this paper. **f** ISAR image gained via azimuth SPWVD transform

shown in Fig. 4d. The correlation coefficient of adjacent range profiles of the terahertz radar data keep above 0.99 and the envelope of terahertz radar echo is very similar. The 1699th pulse echo is selected as the unity benchmark of envelope alignment. The envelope after envelope alignment via the envelope alignment technique proposed in this paper is shown in Fig. 4e. The ISAR image is shown in Fig. 4f with the SPWVD in azimuth imaging.

We can observe that the envelope alignment technique proposed in this paper has a higher envelope alignment accuracy than that the adjacent amplitude correlation method has from Fig. 4b, e. Comparing Fig. 4c, f, a higher quality ISAR image is acquired via the envelope alignment technique proposed in this paper. Because the ISAR image of the maneuvering target in Fig. 4f is generated with the SPWVD transform in azimuth imaging, the azimuth resolution is expanded.

4 Conclusion

In this paper, a novel envelope alignment technique is presented, which solves the problems of jump error and drift error in the conventional adjacent amplitude correlation method. This method is suitable for terahertz radar ISAR imaging of maneuvering targets with a small rotation angle. Experiments have demonstrated the effectiveness of the envelope alignment technique proposed in this paper.

Acknowledgments This work was supported by the National Nature Science Foundation of China under Grants 61271287, 61301265, U1433113.

References

1. Cooper K, Dengler R, Lombart N et al (2011) THz imaging radar for standoff personnel screening. *IEEE Trans Terahertz Sci Technol* 1(1):169–182
2. Gu S, Li C, Gao X et al (2012) Terahertz aperture synthesized imaging with fan-beam scanning for personnel screening. *IEEE Trans Microw Theory Technol* 60(12):3877–3885
3. Chen CC, Andrews HC (1980) Target motion induced radar imaging. *IEEE Trans Aerosp Electron Syst* 16(1):2–14
4. Cheng B, Jiang G, Wang C et al (2013) Real-time imaging with a 140 GHz inverse synthetic aperture radar. *IEEE Trans Terahertz Sci Technol* 3(5):594–605
5. Li X, Liu GJ, Ni L (1999) Autofocusing of ISAR images based on entropy minimization. *IEEE Trans Aerosp Electron Syst* 35(4):1240–1252
6. Chen V, Hao L (1999) Joint time-frequency analysis for radar signal and image processing. *IEEE Signal Process Mag* 16(2):81–93
7. Zhang B, Pi Y, Li J (2015) Terahertz imaging radar with inverse aperture synthesis techniques: system structure, signal processing, and experiment results. *Sens J IEEE* 15(1):290–299